Phase-Separated Microstructures in "All-Acrylic" Thermoplastic Elastomers

Ph. Leclère [1], A. Rasmont [1], J.L. Brédas [1,2], R. Jérôme [3], J.P. Aimé [4], R. Lazzaroni [1*]

[1] Service de Chimie des Matériaux Nouveaux,
Centre de Recherche en Science des Matériaux Polymères (CRESMAP)
Université de Mons-Hainaut, Place du Parc 20, B-7000 Mons (Belgium)

[2] Department of Chemistry, The University of Arizona,
Tucson, Arizona, 85721-0041 (USA)

[3] Centre d'Etude et de Recherche sur les Macromolécules (CERM)
Université de Liège, Sart-Tilman B6, B-4000 Liège (Belgium)

[4] CPMOH, Université de Bordeaux I
351, Cours de la Libération, F-33405 Talence Cedex (France)

SUMMARY: Atomic Force Microscopy (AFM) is used to study the phase separation process occurring in block copolymers in the solid state. Measuring simultaneously the amplitude and the phase of the oscillating cantilever in tapping-mode operation provides the surface topography along with the cartography of microdomains with different mechanical properties. This in turn allows to characterize the organization of the various components at the surface in terms of well-defined morphologies (*e.g.*, spheres, cylinders, or lamellae). Here this approach is applied to a series of symmetric triblock copolymers made of a central elastomeric segment (polyalkylacrylate) surrounded by two thermoplastic sequences (polymethylmethacrylate). The occurrence of microphase separation in these materials and the resulting microscopic morphology are essential factors for determining their potential applications as a new class of thermoplastic elastomers. This paper describes how the surface morphology can be controlled by the molecular structure of the copolymers (volume ratio between the sequences, molecular weight, length of the alkyl side group) and by the experimental conditions used for the preparation of the films. The molecular structure of the chains is fully determined by the synthesis of the copolymers via living anionic polymerization while the parameters that can be modified when preparing the samples are the nature of the solvent and the thermal annealing of the films. Finally, we report on a systematic comparison between images and approach-retract curve data. We show that this experimental comparison allows the origin of the contrast that produces the image to be straightforwardly evaluated. The method provides an unambiguous quantitative measurement of the contribution of the local mechanical response to the image. We show that most of the contrast in the height and phase images is due to variations in local mechanical properties and not in topography.

 CCC 1022-1360/00/$ 17.50+.50/0

Introduction

Progress in the study of nanoscale materials, whether inorganic or organic, has greatly gained from the development of new analytic techniques. In particular, visualization of structures and assemblies has been made easier by the advent of scanning probe microscopies: Scanning Tunneling Microscopy (STM) and Atomic Force Microscopy (AFM) [1].

Our work is based on the use of Tapping-Mode Atomic Force Microscopy (TMAFM) to gain understanding of the supramolecular organization at the surface of films of block copolymers. Because most polymers are non miscible, the different components of block copolymers tend to phase separate into chemically homogeneous domains. However, the presence of the covalent bonds between the different sequences does not allow phase separation to proceed over a large length scale. Instead, only small domains with typical sizes in the range of tens of nanometers can be formed. The relation between the composition and the bulk morphology in diblock copolymers has been determined experimentally by scattering techniques and transmission electron microscopy and is now understood to a large extent [2]. For symmetric compositions (*i.e.*, around 50% in each constituent), the copolymers arrange as an alternating array of lamellae parallel to each other.

The microdomain organization at the surface of block copolymers is a very important issue because the chemical nature of the surface governs its interactions with the surrounding medium and with other materials. Compared to the situation in the bulk, the morphology at the surface is expected to be strongly affected by the presence of the interface with air. Surface segregation phenomena in block copolymers have been intensively studied over the past two decades, mainly with surface-sensitive spectroscopies [3], and more recently with scanning probe techniques [4-5].

This paper describes a systematic AFM study of a series of symmetric triblock copolymers, known as thermoplastic elastomers (TPE). In such compounds, the central segment consists of a rubbery polymer, *i.e.,* its glass transition temperature (Tg) is below room temperature; it is the major component of the copolymer. The outer two blocks are made of a thermoplastic, *i.e.,* a polymer for which the Tg is well above room temperature. Below the Tg of the thermoplastic, the thermoplastic domains are rigid and act as crosslinks within the elastomeric

matrix; the material thus behaves as a vulcanized rubber. Above the melting point of the thermoplastic, both components flow and the material can be processed by usual polymer processing techniques. TPE's are therefore thermoreversible elastomeric materials.

The chemical structure of the copolymers considered in this study is shown in scheme 1. Two identical thermoplastic sequences of poly(methyl methacrylate), PMMA, surround a central sequence of poly(alkyl acrylate); hereafter, these compounds will be denoted MAM. Compared to classical TPE's based on styrene-butadiene-styrene copolymers, the materials studied here show a broader service temperature range (because the Tg of PMMA is higher than that of polystyrene) and increased resistance to oxidation (because the polybutadiene component, which contains reactive C=C bonds, is replaced with a more stable polyacrylate sequence).

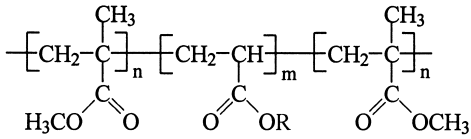

R = ethyl, propyl, *n*-butyl, *i*-octyl

Scheme 1

It is important to realize that TPE properties can be properly obtained only if: (i) the chains of the triblock are very similar in size and composition; this is achieved by careful control of the polymerization procedure [6] using living anionic polymerization; and (ii) microphase separation effectively takes place. In this context, AFM is used to obtain evidence of phase-separated microdomain formation and to determine their assembly on the surface, in connection with the macroscopic mechanical and rheological properties measured independently [7]. It must be stressed that TMAFM appears as a unique tool for investigating the microscopic morphology of such compounds since, on the one hand, the electron density difference between the different monomer units is too small to lead to significant contrast in X-ray scattering measurements and, on the other hand, no selective staining agent is available, which precludes morphological characterization by means of transmission electron microscopy.

In this paper, we first describe the influence of the composition of TPE's on their morphology, as observed with AFM. We then illustrate how morphological transitions can take place at the surface, as a function of the preparation conditions of the copolymer films. Finally, we show

how approach-retract curves can be used to understand the nature of the contrast in topographic and phase TMAFM images.

Experimental section

The MAM triblock copolymers were synthesized by classical anionic polymerization as described elsewhere [7]. Thin copolymer films were cast on freshly-cleaved muscovite mica substrates from dilute solutions in THF or toluene (2mg/ml). The solvent was evaporated slowly over one day at room temperature either in air or in a solvent-saturated atmosphere. The final film thickness was *ca.* 500 nm. This value is ten times larger than the intrinsic pattern period of the materials, which ensures that the morphology is not driven by the assembly on the substrate. The films were kept as such or annealed at 140°C under high vacuum for 24 h before AFM observation.

All the AFM images were recorded with a Nanoscope IIIa microscope from Digital Instruments Inc. in the Tapping Mode (25°C, in air). Microfabricated cantilevers were used with a spring constant of 40 Nm^{-1}. The instrument was equipped with the Extender^{TM} Electronics Module to provide simultaneously height and phase cartography. Images of different areas of each sample were recorded, and the scanning time was *ca.* 5 minutes for most of the images. All the images were collected with the maximum available number of pixels (512) in each direction. For image analysis, the Nanoscope image processing software was used.

Results and Discussion

Microphase separation as observed with TMAFM

Figure 1 shows typical AFM images for the PMMA-*b*-poly(*i*-octylacrylate)-*b*-PMMA (denoted MIM) triblock containing 12.2 wt% PMMA (sample 1, Table 1). In the imaging conditions used here, the height image (Figure 1a) is very uniform, thus indicating that the surface of the analyzed sample is very smooth (the typical value of the root mean square roughness for a 1 x 1 μm^2 area is 1.4 nm). This observation guarantees that the contrast observed in the phase image does not originate from differences in the surface topography and that no tip indentation

into the film occurs. The phase image (Figure 1b) clearly shows a two-phase morphology, which consists of an assembly of bright round-shaped objects in a darker matrix. These objects appear arranged in a regular pattern. Based on what is known of the morphology of block copolymers [8] in this composition range, the AFM phase image can be readily interpreted as spheres of PMMA in a poly(*i*-octylacrylate), PIOA, matrix.

Table 1. Molecular characteristics of the triblock copolymers considered in this study.

Sample	R group	Molecular Weight, M_n (x 10^{-3})	M_w/M_n	% PMMA
1	*i*-octyl	7-100-7	1.07	12.2
2	*i*-octyl	20-140-20	1.04	22.2
3	*i*-octyl	40-140-40	1.06	36.4
4	*n*-butyl	10-50-10	1.05	28.6
5	*n*-butyl	30-150-30	1.05	28.6
6	*n*-propyl	20-90-20	1.06	30.8
7	ethyl	10-50-10	1.09	28.6

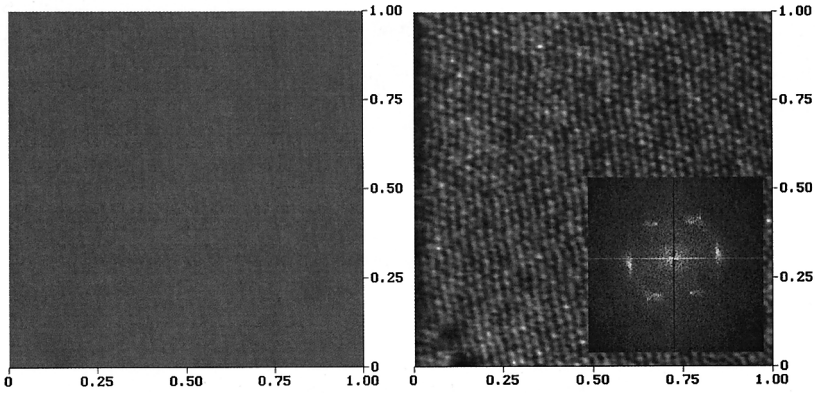

Figure 1. TMAFM height (a) and phase (b) images (1 x 1 μm^2) of a triblock copolymer (sample 1, Table 1). The grayscale of the height image is 10 nm while the phase image shows the morphology of the copolymer. The inset corresponds to the FFT of the phase image and indicates that the PMMA domains are arranged in a hexagonal lattice.

However, it must be stressed that AFM phase images can be interpreted without *a priori* knowledge of the morphology. The phase contrast strongly depends on the details of the tip-sample interactions. In turn, these interactions depend on the intrinsic properties of the analyzed material, in particular its elastic and viscoelastic moduli, but also on the mechanical properties of the tip and on the existence of tip-sample adhesion [9]. Quantitative measurements of the sample mechanical properties on the local scale from TMAFM data are therefore a very delicate task. Nevertheless, a qualitative interpretation of the phase images in terms of the spatial distribution of domains on a heterogeneous surface is possible. Recently, a quantitative approach based on the analytical expressions derived from the non-linear behavior of an oscillating tip-cantilever system was proposed [10]. This theoretical model describes different situations for the oscillating cantilever (non-contact as well as intermittent contact). By fitting the approach-retract curves, it is possible to distinguish the different domains in terms of elastic moduli [11-12]. According to this approach, the bright spots can therefore be assigned to spheres of PMMA, the harder component, thus leading to a larger phase shift, while the darker matrix is made of the softer component (PIOA). These aspects will be discussed in the third part of the paper.

Influence of the composition

The equilibrium phase morphology of block copolymers depends on the copolymer composition. This relationship has been intensively investigated experimentally and rationalized theoretically for styrene-isoprene block copolymers [13]. A spherical morphology is observed for polystyrene (PS) contents lower than 20 vol%; for contents between 20 and 35 vol%, hexagonal arrangement of PS cylinders is observed, whereas a lamellar morphology is reported in the 40-65 vol% range. Finally, for compositions richer in PS, cylindrical and spherical assemblies of polyisoprene are found, as expected. It is also noteworthy that a bicontinuous gyroïd morphology has recently been discovered for compositions intermediate between those leading to cylinders and lamellae [14].

Figure 2 shows the phase images obtained for the three copolymers listed in Table 1. As shown above, for the lowest PMMA content (~12%), the film surface clearly consists of an assembly of bright PMMA spheres in a dark PIOA matrix (Figure 2a). These spheres appear to be arranged in an hexagonal lattice; this surface morphology probably corresponds to a particular face of the body-centered cubic lattice, as expected in this range of composition. Image analysis indicates that the average distance between sphere centers is about 27 nm. Increasing

the PMMA content above 20% (sample 2, Table 1) leads to a morphological transition (Figure 2b). Bright elongated objects exist in a darker continuous matrix. This observation is thought to originate from PMMA cylinders (bright areas) lying parallel to the surface, within the PIOA matrix. The width of the flat cylinders is 19 +/- 1 nm. When the amount of the thermoplastic is further increased, the phase image in Figure 2c is obtained (here, for sample 4, Table 1). The pattern is interpreted as an assembly of alternating thermoplastic and elastomer lamellae, which is consistently with the copolymer composition.

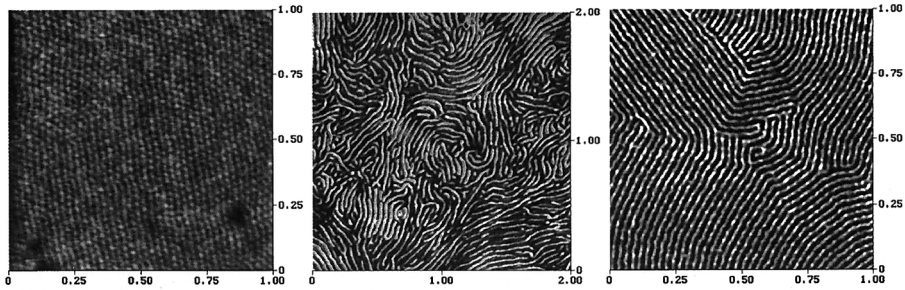

(a) (b) (c)

Figure 2. TMAFM phase images of the triblock copolymers described in Table 1: (a) spherical morphology (sample 1); (b) cylindrical morphology (sample 2); (c) lamellar morphology (sample 4).

As previously explained, the brighter areas that correspond to larger phase values, are typical of the component of higher modulus, *i.e.,* PMMA, whereas the darker areas are the signature of the softer component. Note that the phase image is not reminiscent at all of the topographic profile; it is fully dominated by the local contrast in the mechanical properties, thus constituting clear evidence for microphase separation in this triblock copolymer. Beyond these three examples illustrating the three major morphologies, we have performed a systematic AFM analysis of a larger series of PMMA-*b*-poly(alkyl acrylate)-*b*-PMMA compositions and we have observed in all cases a microdomain morphology consistent with the expectations based on the copolymer composition [8)].

Influence of the sample preparation conditions

Influence of the solvent

The solvent used to prepare the copolymer films can have a deep influence on their morphology, mainly because the solubility of the various components can be slightly different, leading to selective precipitation during the drying process. Here, we have considered two solvents, THF and toluene, which are good solvents for both the thermoplastic block (PMMA) and the elastomer (PIOA). For a given copolymer (sample 2, table 1), we have investigated the surface morphology of films prepared from the two solvents and dried either in open air or in a solvent-saturated atmosphere. Typically, the samples were dried at room temperature for 48 hours. However, due to THF volatility, samples prepared from that solvent and dried in air were ready in a few minutes. The corresponding AFM images are collected in Figure 3.

The films prepared in THF and dried in air (Figure 3a) clearly show the cylindrical morphology already described above. When using a THF-saturated atmosphere or when prepared from toluene, the film surface shows a more complex morphology: cylinders tend to be shorter and a number of bright round-shaped objects are also present at the surface. We believe that these objects are PMMA cylinders standing perpendicular to the surface, so that only their apex is visible; the origin of this change will be interpreted in the discussion section.

In order to obtain a more quantitative description of this evolution, we have performed a grain-size analysis of the images of Figure 3. This operation consists in establishing the distribution of the bright objects according to their size; the corresponding histograms reflect the grain-size distribution. Each class corresponds to an average domain area and the number within the class is the number of domains. A "domain" is defined in terms of conjoined scan lines having a given minimum and maximum size above a certain user-defined threshold. We applied this technique to our phase images. We have focussed on the round-shaped objects considered as cylinders perpendicular to the surface. Their contribution to the total area of the bright domains is negligible (~1%) in Figure 3a; it increases to 22% in Figure 3b, then to 39% in Figure 3c to reach 53% in Figure 3d. The image in Figure 3a is characterized by a distribution decreasing gradually towards the larger areas. In contrast, the domain size distribution computed from Figure 3d displays a well-defined peak around 400 nm^2, due to the large number of small, round-shaped objects. This clearly shows that the solvent used to cast the film and its

evaporation rate strongly influence the surface morphology: fast evaporation of THF leads to cylinders lying flat on the surface while upon slow evaporation of toluene, the cylinders tend to arrange perpendicular to the surface. Beyond the effect of the evaporation rate, the details of the solvent-polymer-air interactions also likely play a role in defining the surface morphology.

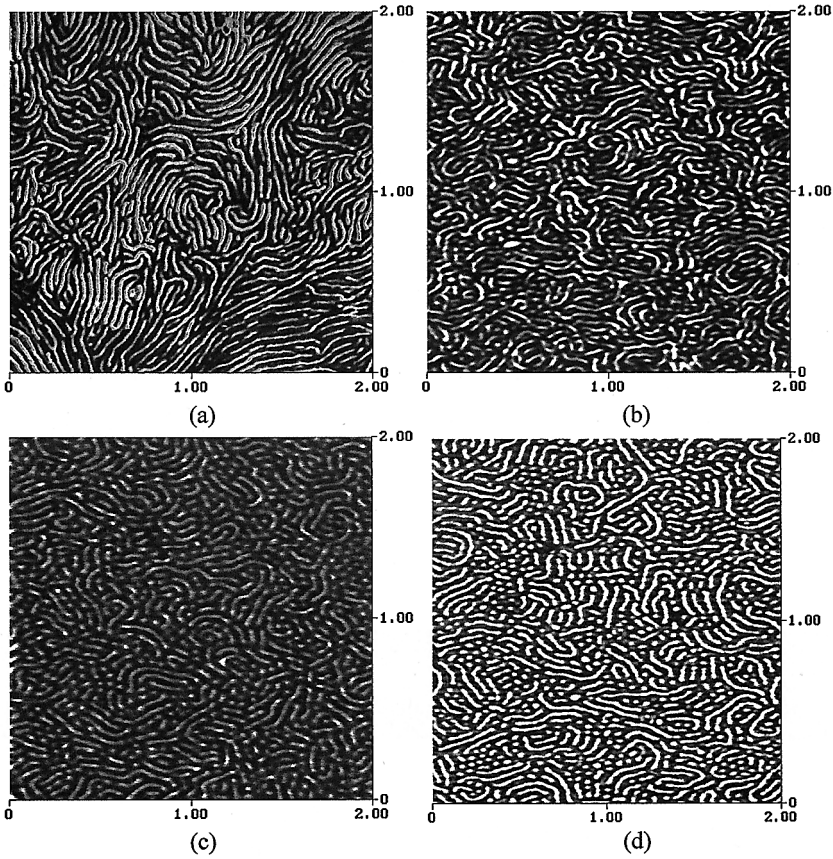

Figure 3. TMAFM phase images of a particular triblock copolymer (sample 2, Table 1): film prepared from THF and (a) dried in air, (b) dried in THF-saturated atmosphere; film prepared from toluene and (c) dried in air, (d) dried in toluene-saturated atmosphere.

Influence of the annealing conditions

Another important parameter expected to influence the morphology of block copolymers is the annealing process. When the sample is annealed to a temperature above the glass transition temperature of the two components, chain mobility is improved and morphological changes

can occur. Images were taken on the same film before and after it had been annealed at 140°C during 24h (we observed that the morphology is not further modified after annealing for 48h, which suggests that after 24 h the situation is close to thermodynamic equilibrium). For the non-annealed sample, the surface consists of a mixture of PMMA cylinders, lying flat and perpendicular to the surface; the width of the flat cylinders (30 +/- 2 nm) is identical to the diameter of the spots corresponding to cylinders standing upright. Annealing significantly modifies the morphology: almost all cylinders become perpendicular to the surface; they now represent 93% of the total area of PMMA domains versus only 53% before annealing.

Interpretation of the morphology

Thus, both the solvent and the annealing process can modify the surface morphology of these triblock copolymers. An explanation for the observed morphologies can be found on the basis of the basic thermodynamic considerations. From our results, it appears that the ratio of standing/flat cylinders tends to increase upon slow evaporation and/or upon annealing. This suggests that the most stable arrangement of the PMMA cylinders is perpendicular to the surface. This is consistent with the higher surface energy of PMMA (42.7 mJ/cm²) compared to PIOA (34.3 mJ/cm²) [15]. The system indeed tends to organize so as to minimize the amount of PMMA at the surface, thus by exposing only the apex of the PMMA cylinders. An aletrnative explanation would be that the cylinder morphology gradually evolves into a spherical morphology, due to the formation of a thin layer of the elastomer (*i.e.*, the lowest surface energy component), covering the whole surface and affecting the local composition ratio. However, preliminary Secondary Ion Mass Spectrometry (SIMS) results show that both components are indeed present at the outer surface, even for the sample of Figure 4c. Moreover, the intimate coexistence of elongated and round-shaped objects also seems incompatible with the presence of a full layer of one component covering the surface. This is why we believe that the transition of flat to upright cylinders is the most reasonable explanation for the evolution observed in Figure 4. In Figure 4b, the sample has probably not reached full thermodynamic equilibrium yet, since flat cylinders are still visible on the surface while in Figure 4c, almost all cylinders are standing and only a few short segments are lying flat on the surface.

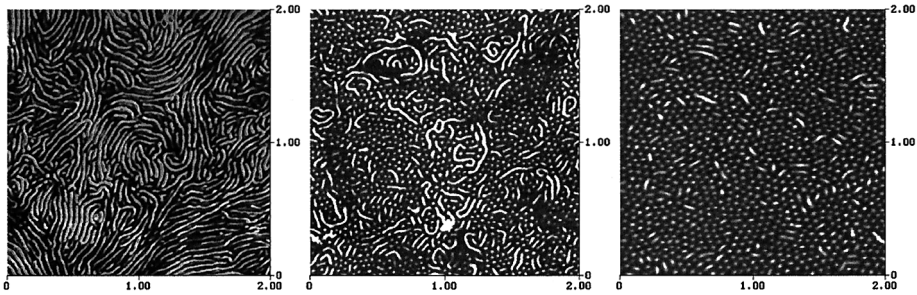

Figure 4. TMAFM phase images of the MIM triblock copolymer corresponding to sample 2 in Table 1, prepared from a THF solution (a) evaporated in air, non annealed; (b) evaporated in air, annealed; (c) evaporated in a THF-saturated atmosphere, annealed.

This evolution is clearly observed in the corresponding domain size distributions. The surface distribution is very broad for the sample evaporated in air and non annealed. On Figure 4a, only 1% of the total area of the PMMA domains corresponds to standing-up cylinders, while this ratio jumps to 41% and 72% for Figure 4b and Figure 4c, respectively. The average surface for the PMMA domains observed all over Figure 4c is about 400 nm^2, which corresponds to cylinders with a diameter of 23 nm. The distribution corresponding to the mixed morphology (Figure 4b) shows a broad peak centered around 700 nm^2; this peak contains the contribution of the standing-up cylinders and the large number of very short flat cylinders, which can be thought of as "bridges" between two cylinders developing downwards perpendicular to the surface. As a result, the size distribution is shifted towards larger areas, relative to the situation where only standing-up cylinders exist (Figure 4c). This mixed morphology can thus result from the interplay between entropic (*i.e.*, surface disordering) and enthalpic (*i.e.*, surface energy) factors. It is reasonable to think that the entropic gain corresponding to the formation of a disordered assembly of cylinders can partly overcome the enthalpic loss of bringing more PMMA to the surface, even at moderate temperatures. It must be noted that mixed arrangements of cylinder has been observed [16].

Increasing the PMMA content in the block copolymers to around 50% leads to the lamellar morphology, as illustrated above. The alternation of dark and bright stripes corresponds to lamellae of the soft and hard components, assembled perpendicular to the surface. The orientation of lamellae in thin films of block copolymers has received considerable attention in

recent years [17]. It has been shown that, under near equilibrium conditions, diblock copolymers exhibit a strong orientation of the lamellae parallel to the surface, with the lamellae lying on top of each other parallel to the substrate; in that case, the films organize in such a way that a lamella of the component with smaller surface energy occupies the outer surface. It has also been shown that orientation occurs at both the air/copolymer and copolymer/substrate interfaces. The surface-induced orientation in solution-cast films was also found to be independent of the thickness of the film [18]. Therefore, under near equilibrium conditions, no perpendicular lamellar structures can be observed at the surface of diblock copolymers. This implies that perpendicular lamellae can only be observed at the surface as defect structures or by confining the films between two rigid surfaces [19]. Recently, Morkved *et al.* have described the possibility to observe perpendicular lamellae but only when the film thickness is exactly one lamellar repeat spacing [20]. When the thickness is larger than one lamellar period, the lowest energy structure in diblock copolymer is always one with lamellae oriented parallel to the free surface (polymer/air interface) of the film.

In our triblock copolymers, a similar arrangement, with only the less polar segments (*i.e.*, the central PIOA sequence) exposed to the surface, would imply that all chains form loops so that both their external PMMA sequences are accommodated in a lamella below the surface. Such an organization corresponds to a significant loss in conformational freedom and is therefore expected to be entropically unfavorable. Instead, in a lamellar arrangement perpendicular to the surface, the central segments can either be extended or looped; this should thus be more favorable entropically. Since the difference in surface energy between the components is rather small, this entropy gain probably overcomes the energetic destabilization due to the presence of the most polar component at the surface. Therefore, this particular lamellar organization is a direct consequence of the specific molecular architecture of these block copolymers and is not related to a thickness effect or to interactions with the substrate.

Influence of the alkyl group in the acrylate units

In this section, we discuss the effect of the length of the alkyl group in the acrylate units of the central segment. We have compared the surface morphology of copolymers with similar PMMA contents and with different alkyl groups : *n*-butyl (nB), *n*-propyl (nP), and ethyl (E). Figure 5a corresponds to the 30000-150000-30000 MnBM copolymer (sample 5, Table 1). As described above, the observed morphology reflects the presence of PMMA cylinders (bright

areas), either standing perpendicular or lying parallel to the surface, within the poly(*n*-butylacrylate) matrix. A similar situation is found in Figure 5b for the 20000-90000-20000 MnPM copolymer (sample 6, Table 1). For high-molecular weight PMMA-*b*-poly(ethylacrylate)-*b*-PMMA copolymers, microphase separation takes place (not shown here). However, with the corresponding low-molecular weight compound (sample 7, Table 1), the AFM phase image is completely featureless, indicating the absence of microphase separation (Figure 5c). This situation is due to the combined effects of the similarity in the chemical structure of the blocks and the low-molecular weight values. These two factors tend to favor mixing over phase separation.

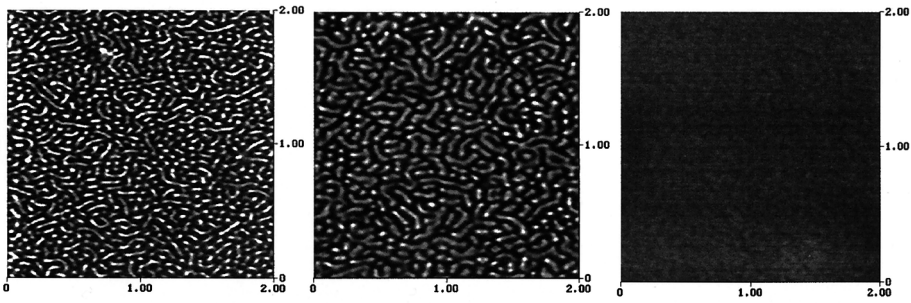

Figure 5. TMAFM phase images of MAM triblock copolymers with different alkyl groups (samples 5-7, Table 1) (a) *n*-butyl, (b) *n*-propyl, and (c) ethyl.

For the same reason, no phase separation is observed for the 10000-50000-10000 MnPM copolymer, whereas the MIM and MnBM copolymers all show microphase separation, independently of their molecular weight. It is essential to notice that the presence or absence of phase separation observed with AFM in this family of materials fully agrees with the mechanical properties analysis described elsewhere [7].

Origin of the contrast in height and phase images

We here address the question of the origin of the contrast in TMAFM images of those triblock copolymers. A number of studies have shown the possibility to extract useful information from the tapping-mode images of soft samples, especially with samples showing a particular contrast at small scale, like blends of hard and soft materials or copolymers [4, 5, 7, 21].

Nevertheless, questions remain about an accurate description of the physical origin of the tapping-mode image contrast [9, 10-12, 22-25]. In many cases, the height images are considered to display topographic information, but it must be kept in mind that the local mechanical properties of the samples may also contribute to contrast in the height image. For the phase images, using the dominant repulsive regime [11] and disregarding the nonlinear deformation of the resonance peak, the phase shifts are related to the local mechanical properties. At this point, it is worth mentioning that, in order to keep a well-defined oscillating behavior of the tip, the perturbation to the oscillator due to the contact with the surface is chosen to be small; in other words, the reduction of the free amplitude (the setpoint) is only of a few percents. This method has two advantages: from an experimental point of view, this allows to identify immediately hard and soft domains, the bright parts of the image corresponding to hard domains [5]; from a theoretical point of view, this allows us to use simple approximations that provide analytical solutions to fit the experimental data [9, 26]. Note that other techniques, such as the pulsed-force mode, could also be used to discriminate between the topographic and mechanical contributions to the image [27].

Practically, when recording approach-retract curves, the sample is moved up and down (on the z direction) at a fixed X,Y location on the surface. The amplitude and phase are recorded as a function of the vertical displacement of the piezoactuator holding the sample. Typical experimental conditions are 0.5 Hz for the vertical movement frequency and 20 nm for the vertical extension. The experiments are performed at an oscillator frequency slightly below resonance, as this makes the sample surface location for the approach-retract curves easier. The distance at which the oscillator bifurcates from the free amplitude (A_0) to a higher one (hereafter called D_{bif}) is connected to the strength of the attractive interaction. To measure and correct the possible drift of the sample holder, height and phase images are then again recorded at the same sample location and same amplitude conditions after the series of approach-retract curves has been recorded. The D_{bif} adjustment allows to selectively extract the mechanical contribution in the contrast between the different domains.

From the amplitude curve, one then checks the vertical position Z_i corresponding to the image fixed amplitude A_i (the set point). Then, from the phase curve, one obtains the corresponding phase noted φ_i . This operation is repeated for all the Y positions: Z_i and ϕ_i values are thus recorded for all Y positions for which the approach-retract curves are measured. One thus obtains plots of the piezoactuator heights (Z_i) and phases (ϕ_i) versus Y sample locations, which

are then compared with the corresponding sections of the tapping-mode height and phase images. Figures 6 a and b represent the area chosen for the image reconstruction, with lamellae oriented nearly perpendicular to the scan direction and a clearly-marked contrast between the domains both in height and phase images. Note that in this case, we have strongly reduced the A_i/A_0 value, compared to the imaging conditions used for the data shown previously. This leads to the appearance of the contrast in the height image.

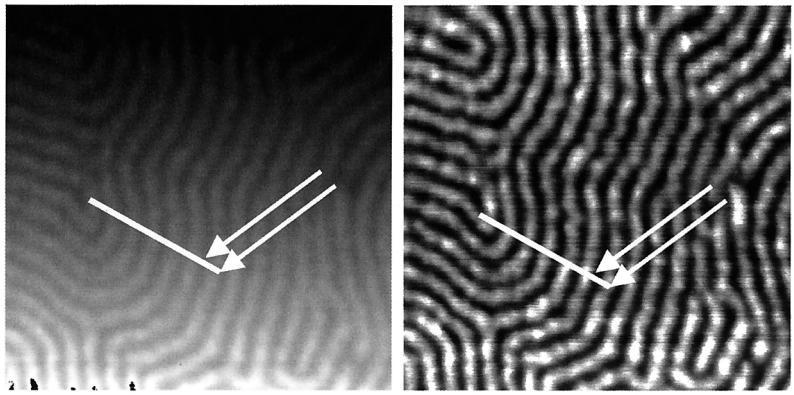

(a) (b)

Figure 6. Tapping-mode images (500 nm x 500 nm) of the area selected for the profile reconstruction: (a) height image (the gray scale is 10 nm), the bright areas corresponding to the upper parts of the image and the dark areas to the lower parts of the image; (b) phase image (the gray scale is 5°). The two white arrows indicate the two areas, corresponding to two different domains, where the approach-retract curves shown in Figure 7 are recorded. The white line corresponds to the section used for the comparison with the section built from the approach-retract curves.

Approach-retract curves recorded on the two spots marked in Figure 6 are represented in Figure 7, giving the amplitude (Figure 7a) and phase variations (Figure 7b). The oscillator responses are clearly different for the two areas. The signature of the glassy domain is represented with gray symbols whereas the elastomer domain corresponds to dark symbols.

The difference in behavior can be attributed to different interactions between the tip and the elastomer and glassy domains. The harder domain (glassy) response has a larger slope than the softer one [11]. Without any topographic consideration, the amplitude variations on the two domains show that for a bifurcation distance set at the same vertical location at a given set-point, the piezoactuator has to move the sample closer to the tip for the elastomer domain than

for the glassy one. Consequently, the net result will be an apparent height higher for the glassy domains. Due to the dominant repulsive regime, the recorded difference is uniquely related to change in slopes of the curves, thus to changes of the local mechanical properties. This latter partly corresponds to the difference in the indentation depth.

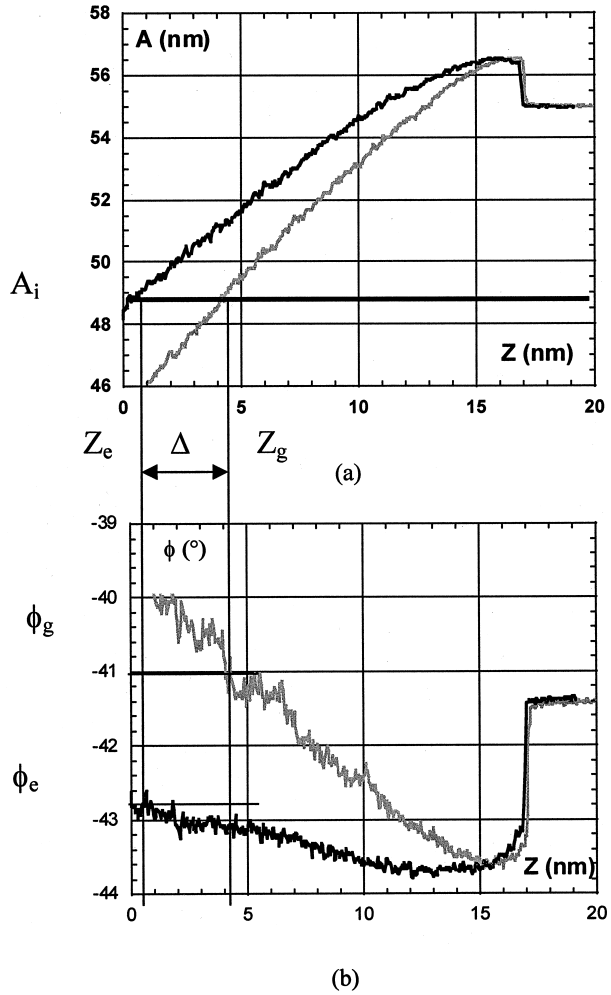

Figure 7. Experimental approach curves recorded on the two spots shown in Figure 6. The results shown in gray (corresponding to the bright areas in Figure 6) relate to the harder, glassy domains and results in black (dark domains of Figure 6) to the softer, elastomer domain: (a) amplitude A variation vs. piezoactuator vertical Z position during the approach; (b) phase ϕ variation vs. piezoactuator vertical Z position during the approach.

The next step is to compare the height and phase image sections with sections built from the approach-retract curve data. The resulting image sections are displayed in Figure 8a (height) and 8b (phase), together with the data from the approach-retract curve analysis. The correspondence between the two sets of data (height or phase images and approach-retract analysis) appears to be very good. This agreement means that for those copolymers, the contrast in the height image is related to different oscillator responses on the glassy and elastomer domains, with no discernible topographic contribution to the contrast. Therefore, the contrast is mostly due to changes in the sample local mechanical properties. The correspondence between the two sets of data in Figure 8 is very good, indicating a major mechanical contribution to the height and phase images.

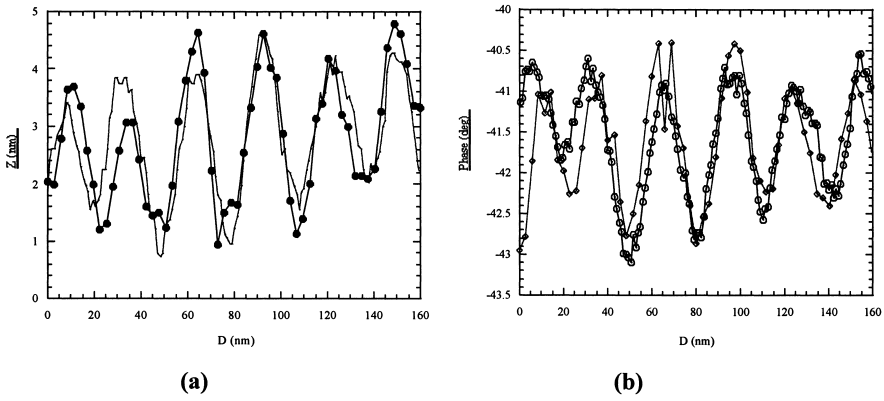

Figure 8. Comparison of the image sections with the profiles built from the approach-retract curves data: (a) height data; (b) phase data. The approach-retract curves have been recorded along the line shown on Figure 6b.

The method applied to that system indicates a major contribution of the mechanical properties to the contrast of the images. It is therefore possible to evaluate experimentally the mechanical and topographic contributions to the tapping-mode images contrast. To achieve such a goal, a number of experimental conditions are required: (i) the tip must be small enough; typically the dominant attractive regime must be achieved for an amplitude as small as 15 nm; (ii) the oscillator must adiabatically scan the sample; (iii) growth of nanoprotuberances has to be prevented and the change in the strength of the attractive interaction between the two domains

must be minimized. The last two points can be easily achieved by choosing a suitable oscillation amplitude such that the oscillator works in the dominant repulsive regime.

Conclusions

The phase morphology of poly(methylmethacrylate)-*b*-poly(alkylacrylate)-*b*-poly(methylmethacrylate) triblock copolymers has been studied by Tapping-Mode atomic force microscopy with phase detection imaging. Spherical, cylindrical, and lamellar morphologies have been observed for block copolymers of increasing PMMA content.

By choosing proper preparation conditions and annealing treatment, the orientation of the cylinders relative to the surface can be modified from a fully-parallel organization to a fully-perpendicular arrangement. The latter is thought to be more stable thermodynamically, since the amount of the most polar component at the surface is minimized. In contrast to the situation in diblock copolymers, lamellae are always found to assemble perpendicular to the surface. This is probably due to the specific molecular architecture of these symmetric triblock copolymers; the entropic loss related to chain folding in the central segment, to form a parallel arrangement, is probably not counterbalanced by the enthalpic gain of removing the most polar component from the surface.

Moreover, the analysis of a series of copolymers based on different alkylacrylates also points to the relation between the molecular structure of the monomers units, the molecular weight of the copolymer and the occurrence of microphase separation, and the resulting thermoplastic elastomers behaviors.

While the proposed procedure for describing the physical origin of the contrast is helpful, it does not bring information about the relative influence of the reactive and dissipative behavior of the sample. To get an accurate description of the mechanical properties requires further developments. In particular, one has to address the difficult question of the modeling of the local dissipation and indentation processes during the intermittent contact situation and their influence on the oscillation behavior.

Acknowledgements

The collaboration between Mons and Liège is conducted in the framework of the Belgian Federal Government Office of Science Policy (SSTC) "*Pôle d'Attraction Interuniversitaire en Chimie Supramoléculaire et Catalyse Supramoléculaire*" (PAI 4/11). Research in Mons is also partly supported by the European Commission and the Government of the Région Wallonne (Project NOMAPOL - Objectif 1 - Hainaut) and the Belgian National Fund for Scientific Research FNRS/FRFC. Research in Bordeaux is supported by the Conseil Régional d'Aquitaine. AR is holder of a doctoral fellowship of "Fonds pour la formation à la Recherche dans l'Industrie et dans l'Agriculture" (FRIA). RL is "Maître de Recherches du Fonds National de la Recherche Scientifique" (FNRS – Belgium).

References

1. R. Wiesendanger, *Scanning Probe Microscopy and Spectroscopy: Methods and Applications*, Cambridge University Press, Cambridge, 1994; S.N. Magonov, M.-H. Whangbo, *Surface Analysis with STM and AFM*, VCH, Weinheim, 1996.
2. B.R.M. Gallot, Adv. Polym. Sc., 29 (1978) 85; B.R.M. Gallot, *In Liquid Crystalline Order in Polymers*, A. Blumstein, Ed.; Academic: New York, 1978, p 223; G. Riess, and P. Bahadur, In *Encyclopedia of Polymer Science and Engineering*, H.F. Mark, N.M. Bikales, C.G. Overberger, G. Menges, Eds.; Wiley: New York, 1989, p 324.
3. P.F. Green, T.M. Christensen, T.P. Russell, R. Jérôme, Macromolecules 22 (1989) 4600; P.F. Green, T.M. Christensen, T.P. Russell, Macromolecules 24 (1991) 252.
4. T.P. Russell, G. Coulon, V.R. Deline, D.C. Miller, Macromolecules, 22 (1989) 2189; G. Coulon, B. Collin, D. Ausserre, D. Chatenay, and T.P. Russell, J. Phys France 51 (1990) 2801; B. Collin, D. Chatenay, G. Coulon, D; Ausserre, and Y. Gallot, Macromolecules 25 (1992) 1621.
5. Ph. Leclère, R. Lazzaroni, J.L. Brédas, J.M. Yu, Ph. Dubois, R. Jérôme, Langmuir 12 (1996) 4317.
6. G. Moineau, M. Minet, Ph. Dubois, Ph. Teyssié, T. Senninger, R. Jérôme Macromolecules, 32, (1999) 27; G. Moineau, M. Minet, R. Jérôme, Macromolecules, 32, (1999) 8277.

7. J. D. Tong, Ph. Leclère, A. Rasmont, J.L. Brédas, R. Lazzaroni and R. Jérôme, *submitted for publication*; A. Rasmont, Ph. Leclère, C. Doneux, G. Lambin, J.D. Tong, R. Jérôme, J.L. Brédas, R. Lazzaroni, Colloids and Surfaces B: Biointerfaces, 19 (2000), 381.
8. F. S. Bates, G. H. Fredrickson, in *Thermoplastic Elastomers*, 2nd edition, G. Holden, N. R. Legge, R. Quirk, H. E. Schroeder, Eds., Hanser: Munich, Vienna, New York, 1996, p. 335.
9. G. Bar, Y. Thomman, R. Brandsch, H.J. Cantow, M.H. Whangbo, Langmuir, 13 (1997) 3807; N.A. Burnham, O.P. Behrend, F. Oulevey, G. Gremaud, P.J. Gallot, D. Gourdon, E. Dupas, A.J. Kulik, H.M. Pollock, G.A.D. Briggs, Nanotechnology, 8 (1997) 67; J.P. Cleveland, B. Anczykowski, A.E. Schmid and, V.B. Elings Appl. Phys. Lett., 72 (1998) 2613; S.N. Magonov, V. Elings, M.H. Whangbo, Surf. Science, 375 (1997) L385; B. Anczykowski, J.P. Cleveland, D. Krüger, V. Elings, H. Fuchs, Appl. Phys. A 66 (1998) S885.
10. S. Kopp-Marsaudon, L. Nony, D; Michel, J.P. Aimé, in *Microstructure and Microtribology of Polymer Surfaces*, ACS Symposium Series 741, V. V. Tsukruk and K. J. Wahl Editors, 2000, chap.8; R. Boisgard, D. Michel, J.P. Aimé, Surf. Science, 401 (1998) 199; J.P. Aimé, D. Michel, R. Boisgard, and L. Nony Phys. Rev., B 59 (1999) 2407;
11. L. Nony, R. Boisgard, J.P. Aimé, J. Chem. Phys., 111 (1999), 1615.
12. S. Kopp-Marsaudon, Ph. Leclère, F. Dubourg, R. Lazzaroni, J.P. Aimé, Langmuir, 16 (2000), 8432.
13. M.W. Matsen, M. Schick Phys. Rev. Lett., 72 (1994) 2660; M.W. Matsen, M. Schick Macromolecules, 27 (1994) 6761; A.K. Khandpur, S. Förster, F.S. Bates, I.W. Hamley, A.J. Ryan, W. Bras, K. Almdal, K. Mortensen, Macromolecules, 28 (1995) 8796.
14. D.A. Hadjuk, P.E. Harper, S.M. Gruner, C. Honecker, G. Kim, E.L. Thomas, L.J. Fetters, Macromolecules, 27, (1994) 4063; M.F. Schultz, F.S. Bates, K. Almdal, K. Mortensen, Phys. Rev. Lett., 73 (1994) 86; A. Avgeropoulos, B.J. Dair, N. Hadichristidis, and E.L. Thomas Macromolecules, 30 (1997) 5434.
15. D.W. Van Krevelen, *Properties of Polymers*, 3rd Ed. Elsevier, Amsterdam (1990), 790.
16. M.A. Van Dijk, R. Van den Berg, Macromolecules, 28 (1995) 6773; G.C.L. Wong, J. Commandeur, H. Fisher, W.H. de Jeu, Phys. Rev. Lett., 77 (1996) 5221.
17. S.H. Anastasiadis, T.P. Russell, S.K. Satija, C.F. Majkrzak, C.F. Phys. Rev. Lett., 62 (1989) 1852; B.L. Carvalho, E.L. Thomas, Phys. Rev. Lett., 73 (1994) 3321.
18. T.P. Russell, G. Coulon, V.R. Deline, D.C. Miller, Macromolecules, 22 (1989) 2189.

19. G.J. Kellogg, D.G. Walton, A.M. Mayes, P. Lambooy, T.P. Russell, P.D. Gallagher, S.K. Satija, Phys Rev. Lett., 76 (1996) 2503.
20. T.L. Morkved, H.M. Jaeger, Europhys. Lett., 40 (1997) 643.
21. J.D. Tong, Ph. Leclère, C. Doneux, J.L. Brédas, R. Lazzaroni, R. Jérôme, Polymer, 41(2000) 4617.
22. J. Tamayo, R. Garcia, Appl. Phys. Lett., 73 (1998), 2926; J. Tamayo, R. Garcia, Appl. Phys. Lett., 71 (1997), 2394.
23. D. Michel, PhD thesis, Université Bordeaux I, 1997, n°1812.
24. L. Wang, Appl. Phys. Lett., 71 (1998), 2394.
25. G.D. Haugstadt, J.A. Hammerschmidt, W.L. Gladfelter in *Microstructures and Tribology of Polymer Surfaces*, ACS Boston, 1998; Haugstad G.; Jones, J. *Ultramicroscopy*, **1999**, *76*, 79.
26. F. Dubourg, S. Kopp-Marsaudon, J.P. Aimé, *in preparation.*
27. N.A. Burnham, A.J. Kulik, G. Gremaud, G.A.D. Briggs, Phys. Rev. Let., 74 (1995), 5092.